

Jet-quenching parameter \hat{q} in the nonperturbative region

Seung-il Nam*

Department of Physics, Pukyong National University (PKNU), Busan 608-737, Republic of Korea

(Dated: January 21, 2014)

We investigate the jet-quenching parameter \hat{q} for the quark-gluon plasma (QGP) for $N_c = 3$, defined nonperturbatively with the Wilson loop in the light-cone (LC) coordinate, at finite temperature (T). Considering the effective static (heavy) quark-antiquark potential $V_{\bar{Q}Q} = \sigma L + C - A/L$, where L indicates the LC transverse separation between the quarks, we obtain $\hat{q} \approx 8V_{\bar{Q}Q}/L^2$. The T dependences for L and other relevant parameters are extracted from the T -dependent instanton (trivial-holonomy caloron) length parameters and the lattice QCD data. By choosing $L \approx a \approx \bar{\rho}_T$, in which a and $\bar{\rho}_T$ denote the lattice spacing and the T -dependent average (anti)instanton size, respectively, we acquire numerically that $\hat{q} = (5 \sim 25)$ GeV/fm for $T = (0 \sim 0.6)$ GeV, and these values are well consistent with other estimations from AdS/CFT and experimental analyses. It turns out that \hat{q} is produced almost by the Coulomb and constant potentials of $V_{\bar{Q}Q}$. We also observe that the ratio T^3/\hat{q} turns into being saturated to $\sim 4.45 \times 10^{-2}$ for $T \gtrsim 0.4$ GeV, indicating the strongly-coupled QGP, and \hat{q} behaves proportionally to T^3 for high T .

PACS numbers: 11.10.Wx, 11.30.Rd, 12.38.-t, 12.38.Mh.

Keywords: Jet-quenching parameter \hat{q} , nonperturbative region, Wilson loop, effective static quark-antiquark potential, liquid instanton model, finite temperature, caloron solution.

The heavy-ion collision experiments, which have been carried out in the Relativistic Heavy-Ion Collider (RHIC) at the Brookhaven National Laboratory (BNL) and the Large Hadron Collider (LHC) of the European Organization for Nuclear Research (CERN) for instance, are a unique place to explore the various nontrivial phenomena of Quantum Chromodynamics (QCD). It has been reported that a highly hot and dense matter is produced during the very short time after the collision: The quark-gluon plasma (QGP). From the comparison between theory of the relativistic hydrodynamic calculation and experiments [1] for the Fourier coefficient of the elliptic flow, the QGP is now believed as an almost perfect fluid, being indicated by the small shear viscosity-to-entropy density ratio $\eta/s \geq 1/(4\pi)$, known as the Kovtun-Son-Starinets (KSS) bound [2]. In Ref. [3], a significant charge separation was observed in the presence of the strong magnetic field, and this was interpreted theoretically in terms of the Chiral Magnetic Effect (CME) [4]. In addition, it is worth mentioning that there appears a suppression of the hadrons in the high- p_T , i.e. medium modification of the parton fragmentation, and this phenomenon can be understood by the so-called *jet quenching*, which amounts the radiative energy loss of the multiple scattering of the partons [5–8]. Hence, the strength of the jet quenching in the medium can be quantified by defining the Jet-Quenching Parameter (JQP) \hat{q} . This physical quantity is also employed as a physical parameter in the hydrodynamic simulations for the heavy-ion collisions. We take notice of that \hat{q} has been investigated theoretically and phenomenologically from various points of view so far. A perturbative definition for \hat{q} was suggested in Ref. [5] in terms of the light-cone correlation of the gluon field strength tensors. In that work, the ratio of T^3/\hat{q} was taken into consideration as a more broadly-valid measure

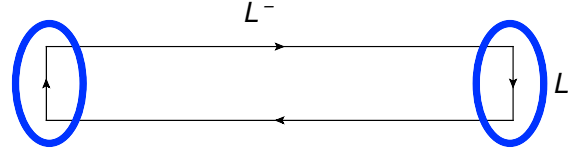


FIG. 1: Light-cone Wilson loop with the light-cone (LC) distance L^- and LC transverse $\bar{Q}Q$ separation L [6]. The ellipse indicates the spatial distribution of the instanton with its size $\bar{\rho} \approx 1/3$ fm.

than η/s , and gives a criteria that $\eta/s (\approx, \gg) 1.25 T^3/\hat{q}$ for the (weakly, strongly) coupled medium. In Ref. [9], the three-dimensional fluid dynamics was performed for the most central Au+Au collision at the next-to-leading (NLO) twist, resulting in $\hat{q} = (1 \sim 2)$ GeV²/fm with the initial time ~ 1 fm and $T \approx 400$ MeV. A nonperturbative definition for \hat{q} was developed by employing the vacuum expectation value (VEV) of the closed contour Wilson loop in the light-cone frame in terms of the dipole approximation [6]. With the nonperturbative definition for \hat{q} , several works in the context of the gauge/string duality, also known as the AdS/CFT, computed \hat{q} : The hot $\mathcal{N} = 4$ supersymmetric QCD [6], medium with chemical potential [10], and bulk geometry with the hyperscaling violation [11]. All of these AdS/CFT approaches showed that $\hat{q} = (3 \sim 20)$ GeV²/fm for $T = (250 \sim 500)$ MeV, showing the tendency that \hat{q} is proportional to T^3 . In the present work, we investigate \hat{q} for the quark-gluon plasma (QGP) for $N_c = 3$, defined nonperturbatively with the Wilson loop in the light-cone (LC) coordinate, at finite temperature (T). To this end, we will utilize the effective static (heavy) quark-antiquark potential with help of the lattice QCD (LQCD) information and T -dependent instanton model.

Firstly, we start by introducing the present theoretical framework for computing \hat{q} in brief. The Wilson loop in a closed contour \mathcal{C} can be described with the number of color N_c as follows:

$$W(\mathcal{C}) = \frac{1}{N_c} \left\langle \text{Tr} \left[\mathcal{P} \exp \left[i \oint_{\mathcal{C}} g_s A_\mu(x) dx^\mu \right] \right] \right\rangle, \quad (1)$$

where \mathcal{P} , g_s and A_μ indicate the path-ordering operator, the gauge coupling and field for the $SU(N_c)$ gauge group. In Ref. [6], \hat{q} was defined nonperturbatively in the static medium, in terms of the VEV of the LC Wilson loop in the *adjoint* (A) representation, which is closed by the LC contour, i.e. $\mathcal{C} = \text{LC}$, as shown in Fig. 1:

$$\langle W_A(\text{LC}) \rangle = \exp \left[-\frac{1}{4\sqrt{2}} \hat{q} L^- L^2 \right] + \mathcal{O} \left(\frac{1}{N_c^2} \right). \quad (2)$$

Here, L and L^- represent the transverse separation between the (heavy) quarks and the LC distance, respectively, satisfying the hierarchy $L \ll L^-$. Note that L also corresponds to the size of the color dipole. They are related to transverse (r) and longitudinal (Δz) distances in the following way [6]:

$$L = \sqrt{\Delta x^2 + \Delta y^2} \equiv r, \quad L^- = \sqrt{2} \Delta z. \quad (3)$$

Being together with this setup, the closed area for the LC Wilson loop can be taken into account as one of the $\frac{\pi}{4}$ -tilted Wilson loops in Euclidean space [12], resulting in

$$s_{\text{LC}} = \frac{1}{\sqrt{2}} L L^-. \quad (4)$$

Secondly, the VEV of an effective LC wilson loop can be constructed from the LQCD and operator product expansion (OPE) information. It is well-known that the static (heavy) quark-antiquark potential can be approximated as the sum of Coulomb, linear, and constant potentials:

$$V_{Q\bar{Q}}(r) = -\frac{A}{r} + \sigma r + C. \quad (5)$$

The values for σ , A , and C were estimated using the quenched LQCD as follows [13]:

$$\sigma a^2 = 0.1629, \quad A = 0.2793, \quad C a = 0.6203. \quad (6)$$

Here, a and σ stand for the lattice spacing and string tension. In Ref. [14], it was also studied that the Wilson loop can be interpreted with the gluon condensate, which is an important order parameters for the nonperturbative QCD, in terms of the OPE:

$$\langle W(\mathcal{C}) \rangle = \frac{2}{zs_C} J_1(zs_C) = 1 - \frac{z^2 s_C^2}{8} + \dots, \quad (7)$$

where $z^2 \equiv \frac{2\pi^2}{3N_c} \mathcal{G}$, in which $\mathcal{G} \equiv \langle \frac{\alpha_s}{\pi} G^2 \rangle$ stands for the gluon condensate. In the vacuum, we have $\mathcal{G}_0 \approx (0.33 \pm$

$0.04)^4 \text{ GeV}^4$ [15]. Although the expression for the Wilson loop in Eq. (7) does not satisfy the positivity of VEV in the large $z^2 s_C^2$ region, we speculate that the effective Wilson loop follows the asymptotic behavior of Eq. (7) for $s_C \rightarrow 0$. Taking into account the above discussions, from a phenomenological point of view, we suggest an effective Wilson loop as follows in the *fundamental* (F) representation up to $\mathcal{O}(s_C^2)$ in Euclidean space:

$$\langle W_F(\mathcal{C}) \rangle = \exp \left[-C\tau - \left(\sigma - \frac{A}{r^2} \right) s_C - \frac{z^2 s_C^2}{8} \right], \quad (8)$$

where $\tau r = s_C$. Eq. (8) satisfies that $\langle W_F(\mathcal{C}) \rangle$ becomes unity $\tau \rightarrow 0$, and $-\lim_{\tau \rightarrow \infty} \frac{1}{\tau} \ln[\langle W_F(\mathcal{C}) \rangle] = V_{\bar{Q}Q}$ for the small s_C . Using Eqs. (3) and (4), and considering that $\ln \langle W_A(\mathcal{C}) \rangle = 2 \ln \langle W_F(\mathcal{C}) \rangle$ [6], we can rewrite Eq. (8) in the LC coordinate as follows:

$$\begin{aligned} \langle W_A(\text{LC}) \rangle = \exp & \left[-\sqrt{2} C L^- - \sqrt{2} \left(\sigma - \frac{A}{L^2} \right) L^- L \right. \\ & \left. - \frac{z^2}{8} (L^- L)^2 \right]. \end{aligned} \quad (9)$$

Then, by equating Eqs. (2) and (9) up to leading large- N_c contributions and $\mathcal{O}(s_{\text{LC}}^2)$, one is led to

$$\hat{q} = \sum_{n=0}^3 \hat{q}_n \left(\frac{1}{L^n} \right) = \frac{1}{\sqrt{2}} z^2 L^- + \frac{8\sigma}{L} + \frac{8C}{L^2} - \frac{8A}{L^3}. \quad (10)$$

As will be shown later, since the contribution from the first term $\hat{q}_0 \propto L^-$ is relatively negligible, by comparing Eq. (5) with Eq. (10), we obtain a simple and useful relation between \hat{q} and $V_{\bar{Q}Q}$:

$$\hat{q} \approx \frac{8V_{\bar{Q}Q}}{L^2}. \quad (11)$$

Since we are interested in computing \hat{q} at finite T , it is necessary to modify all the relevant variables, z , L^- , L , σ , and so on in Eq. (10) as functions of T . For this purpose, we want to employ the LQCD data and the modified liquid-instanton model (mLIM). In this model, which is properly defined in Euclidean space, all the relevant instanton parameters, such as the average inter-(anti)instanton distance \bar{R} and average (anti)instanton size ($\bar{\rho}$), are given as functions of T , using the trivial caloron solution, i.e. Harrington-Shepard caloron, as the compactified instanton solution through the Euclidean temporal direction [16–18]. An instanton distribution function for arbitrary N_c can be written with a Gaussian suppression factor as a function of T and an arbitrary instanton size ρ for the pure-gluon QCD, i.e. Yang-Mills equation in Euclidean space [17]:

$$\begin{aligned} d(\rho, T) &= C \rho^{b-5} \exp \left[-\mathcal{F}(T) \rho^2 \right], \\ \mathcal{F}(T) &= \frac{1}{2} A_{N_c} T^2 + \left[\frac{1}{4} A_{N_c}^2 T^4 + \frac{\nu \bar{\beta} \gamma}{\bar{R}^4} \right]^{\frac{1}{2}}. \end{aligned} \quad (12)$$

Note that the CP -invariant vacuum was taken into account in Eq. (12), and we assumed the same analytical form of the distribution function for the (anti)instanton. The instanton packing fraction $1/\bar{R}^4$ and $\bar{\rho}$ are functions of T implicitly here. The notations read for $N_c = 3$ as follows:

$$A_{N_c} = \frac{3}{2}\pi^2, \quad \gamma = \frac{81}{32}\pi^2, \quad b = 11, \quad \nu = \frac{7}{2}. \quad (13)$$

Using the instanton distribution function in Eq. (12), we can compute the average value of the instanton size $\bar{\rho}^2$ straightforwardly as a function of T as follows [19]:

$$\bar{\rho}_T^2 \equiv \bar{\rho}^2(T) = \frac{[A_{N_c}^2 T^4 + 4\nu\bar{\beta}\gamma n]^{\frac{1}{2}} - A_{N_c} T^2}{2\bar{\beta}\gamma n}. \quad (14)$$

It is clear that Eq. (14) satisfies the following asymptotic behavior [19]:

$$\lim_{T \rightarrow \infty} \bar{\rho}_T^2 = \frac{\nu}{A_{N_c} T^2}, \quad (15)$$

which shows a correct scale-temperature behavior at high T , i.e., $1/\bar{\rho} \propto T$, since $1/\bar{\rho}$ is characterized as the renormalization scale of mLIM: $\Lambda_{\text{mLIM}} \approx 600$ MeV in the vacuum [17]. We can also compute the instanton packing fraction $1/\bar{R}^4$ or the instanton number density n by solving the following equation:

$$n^{\frac{1}{\nu}} \mathcal{F}(T) = [\mathcal{C} \Gamma(\nu)]^{\frac{1}{\nu}}, \quad (16)$$

where $\Gamma(\nu)$ stands for the Gamma function with the argument ν . Note that $1/\bar{R}^4 = n$ is a function of T implicitly: $\bar{R}_T \equiv \bar{R}(T)$ and $n_T \equiv n(T)$. By equating Eqs. (12) and (16), we have $\bar{\beta} = \nu/(\gamma\bar{\rho}^4 n)$. For simplicity, we determine the value of $\bar{\beta}$ at $T = 0$: $\bar{\beta} = \nu/(\gamma\bar{\rho}_0^4 n_0)$. Similarly, the coefficient \mathcal{C} becomes $n_0(\nu\bar{\beta}\gamma n_0)^{\nu/2}/\Gamma(\nu)$. It is worth mentioning that n corresponds to the gluon condensate in a convenient form: $\frac{1}{\bar{R}^4} = n = \frac{1}{8}\mathcal{G}$. Considering all the ingredients above, we can obtain the T dependences of the relevant parameters, i.e. $\bar{\rho}_T$, n_T , and \bar{R}_T , numerically, as shown in the left panel of Fig. 2. At $T = 0$, we have $\bar{\rho}_0 = 0.345$ fm, $n_0 = 1.625 \times 10^{-3} \text{ GeV}^4$, and $\bar{R}_0 \approx 1.020$ fm, giving the gluon condensate $\mathcal{G}_0 = 0.013 \text{ GeV}^4$, which is well consistent with the phenomenological value [15]. Note that here is a *hierarchy* in the length parameters $\bar{\rho}_T \ll \bar{R}_T$, and their discrepancy becomes more obvious as T increases as shown in the figure. The curve for $\bar{\rho}_T$ indicates that the average (anti)instanton size smoothly decreases with respect to T , and inversely for \bar{R}_T . This tendency shows that the instanton ensemble becomes diluted and the nonperturbative effects from the quark-instanton interactions are diminished. Taking into account that the instanton size corresponds to the renormalization scale of the present model, i.e. UV cutoff mass, $\bar{\rho} \approx 1/\Lambda_{\text{mLIM}}$, the T -dependent cutoff mass is a clearly distinctive feature in comparison to other low-energy effective models, such as the NJL model. We also

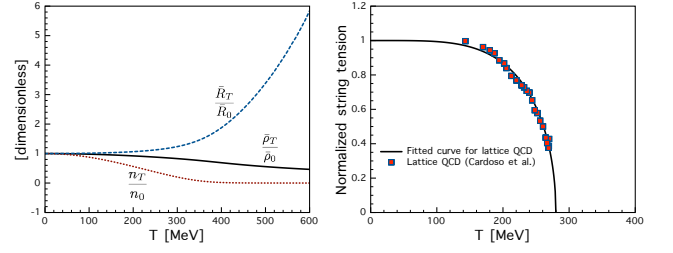


FIG. 2: (Color online) Left: $\bar{\rho}_T/\bar{\rho}_0$ (solid), $\mathcal{G}_T/\mathcal{G}_0$ (dot), and \bar{R}_T/\bar{R}_0 as functions of T . Right: Normalized string tension from the LQCD simulation [20] (square), its parameterization (solid).

show $n_T/n_0 = \mathcal{G}_T/\mathcal{G}_0$ there. As observed, the gluon condensate, $\mathcal{G}_T = 8n_T$ decreases with respect to T , indicating the partial chiral restoration, being similar to that of $\bar{\rho}_T$. We also note that the gluon condensate small but remains finite beyond $T \approx 300$ MeV. Considering that the nonperturbative effects are generated by the instanton contributions and their hierarchies in the length parameters, the LC lengths, L and L^- , are assumed to be in the relations that $\bar{\rho}_T \approx L$ and $\bar{R}_T \approx L^-/\sqrt{2}$, using Eq. (3), as shown in Fig. 1. As for the T dependence of the string tension σ_T , we used it from the LQCD data [20] as shown by the square in the right panel of Fig 2, and parameterize it with $(\sigma/\sigma_0)^2 = 1 - [(T - T_0)/T_C]^4$ for $(T_0, T_C) = (10, 280)$ MeV, given by the solid line. Since $\bar{\rho}_T$ relates to the cutoff scale $\sim \Lambda_{\text{mLIM}}$, it is natural to choose the lattice spacing as $a \approx \bar{\rho}_T$. Due to this choice, the value for σ_0 is chosen to be 0.27 GeV/fm with Eq. (6) and $a \approx \bar{\rho}_0 = 0.345$ fm. Note that this value is smaller than the phenomenological one $\sigma_0 = 0.89 \text{ GeV/fm}$ for $a = 0.19$ fm [13]. It is also interesting to see the asymptotic behavior of \hat{q} as $T \rightarrow \infty$. Using Eqs. (10) and (15), and ignoring \hat{q}_0 , then we have a simple expression as follows:

$$\hat{q}_\infty \approx 8V_{\bar{Q}Q}\pi^3 \left(\frac{11N_c - 6}{33N_c - 36} \right)^{\frac{3}{2}} T^3, \quad (17)$$

which gives $\hat{q}_\infty \approx 177.743 \times T^3 [\text{GeV/fm}]$ for $N_c = 3$ with Eq. (6).

Now, we are in a position to present the numerical results for \hat{q} with relevant discussions. In the left panel of Fig. 3, we present the numerical results separately for each \hat{q}_n in Eq. (10), in addition to the total result. We note that \hat{q}_0 with the gluon condensate (dot) is almost negligible in comparison to others. Similarly, \hat{q}_1 corresponding to the string tension (long-dash) gives only small contribution and is terminated at $T \approx 280$ MeV by construction from the LQCD data, as depicted in the left panel of Fig. 2. In contrast, \hat{q}_2 (short-dash) and \hat{q}_3 (dot-dash), which are proportional to the Coulomb and constant potentials in Eq. (5), respectively, present dominant contributions in the opposite way, and their delicate com-

petition makes difference, being led to the total \hat{q} (thick-solid). We notice an increasing curve for \hat{q} with respect to T and come by numerically that $\hat{q} = (5 \sim 25)$ GeV/fm for $T = (0 \sim 0.6)$ GeV. The parameterization of \hat{q} for $T \rightarrow \infty$ in Eq. (17) is also drawn in the thin-solid line. We also demonstrate other theoretical results: The narrow diamond, inverted-triangle, square, diamond, circle, and triangle symbols designate the theoretical results from the NLO three-dimensional fluid dynamics [9], stochastic QCD [21], SU(2_c) LQCD simulation [22], AdS/CFT with the case-II hyperscaling violation [11], AdS/CFT for $\mathcal{N} = 4$ supersymmetric QCD [23], and AdS/CFT with chemical potential [10]. The shaded area stands for the time-averaged \hat{q} , extracted from the RHIC experiment [24, 25]. By comparing ours with other results, it turns out that our numerical results are well consistent with those from the AdS/CFT results, whereas the LQCD and other theoretical results are relatively smaller than ours. This observation tells us that our numerical result for \hat{q} becomes proportional to T^3 as T increases, as explicitly shown in Eq. (17), being similar to that all the AdS/CFT estimations do as $\hat{q}_{\text{SYM}} = \frac{\pi^2 \sqrt{\lambda}}{a} T^3$ [23]. For $T = (300 \sim 500)$ MeV, our result agrees with the time-averaged \hat{q} of RHIC [24, 25]. In Ref. [5], it was discussed that the relation between the ratio T^3/\hat{q} defines the strong- or weak-coupling region with the shear viscosity-to-entropy density ratio η/s as follows:

$$\frac{\eta}{s} (\approx, \gg) 1.25 \frac{T^3}{\hat{q}} : (\text{weak, strong}) \text{ coupling.} \quad (18)$$

Note that there appeared the Kovtun-Son-Starinets (KSS) bound, signaling the QGP as an almost perfect fluid [2]: $\frac{\eta}{s} \geq \frac{1}{4\pi}$. We evaluate T^3/\hat{q} and show the results in the right panel of Fig. 3. We also depict the KSS bound/1.25 in the figure (thin-solid). It turns out that the curve (thick-solid) increases up to $T \approx 400$ MeV, then gets saturated to $\sim 4.45 \times 10^{-2}$ beyond it. Again, this tendency indicates that $\hat{q} \propto T^3$ at the high- T region. In comparison to the KSS bound, our values are about (30 ~ 50)% smaller, so that the T region, which we are interested in with the instanton framework, denotes possibly the strongly-coupled QGP as expected.

We make a brief summary: The jet-quenching parameter \hat{q} has been scrutinized for $N_c = 3$ in the nonperturbative region, employing the effective static (heavy) quark-antiquark potential with the help of the LQCD data and T -dependent instanton length parameters, providing a neat expression $\hat{q} \approx 8V_{\bar{Q}Q}/L^3$ and showing the tendency $\hat{q} \propto T^3$ for high T . We arrived at an approximated expression for it, i.e. $\hat{q} \approx 177.743 T^3$ [GeV/fm] as T goes infinity. The numerical results are well consistent with other theoretical and experimental analyses, especially from those from AdS/CFT. It also turned out that the Coulomb and constant potentials of $V_{\bar{Q}Q}$ play a most important role to produce \hat{q} . Now, we are planning to derive the relation between η/s and T^3/\hat{q} in a consistent

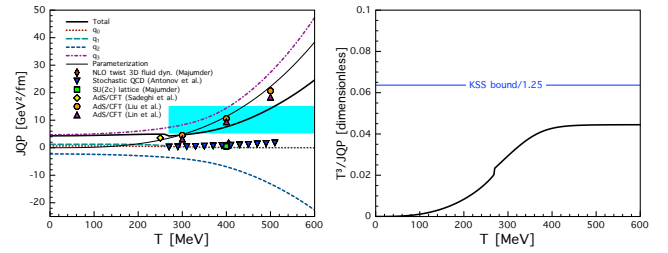


FIG. 3: (Color online) Right: Jet-quenching parameter (JQP) \hat{q} in Eq. (10) as a function of T . Left: T^3/\hat{q} as a function of T . See the text for details.

way to see whether the system is indeed characterized by the strongly-coupled QGP. Related works are under progress and will appear elsewhere.

* E-mail: sinam@pknu.ac.kr

- [1] H. Song *et al.*, Phys. Rev. Lett. **106**, 192301 (2011) [Erratum-ibid. **109**, 139904 (2012)].
- [2] P. Kovtun, D. T. Son and A. O. Starinets, Phys. Rev. Lett. **94**, 111601 (2005).
- [3] B. I. Abelev *et al.* [STAR Collaboration], Phys. Rev. Lett. **103**, 251601 (2009).
- [4] K. Fukushima, D. E. Kharzeev and H. J. Warringa, Phys. Rev. D **78**, 074033 (2008).
- [5] A. Majumder, B. Muller and X. N. Wang, Phys. Rev. Lett. **99**, 192301 (2007).
- [6] H. Liu, K. Rajagopal and U. A. Wiedemann, JHEP **0703**, 066 (2007).
- [7] M. Benzke, N. Brambilla, M. A. Escobedo and A. Vairo, JHEP **1302**, 129 (2013).
- [8] A. Buchel, Phys. Rev. D **74**, 046006 (2006).
- [9] A. Majumder, C. Nonaka and S. A. Bass, Phys. Rev. C **76**, 041902 (2007).
- [10] F. L. Lin and T. Matsuo, Phys. Lett. B **641**, 45 (2006).
- [11] J. Sadeghi and S. Heshmatian, arXiv:1308.5991 [hep-th].
- [12] H. J. Pirner and N. Nurpeissov, Phys. Lett. B **595**, 379 (2004).
- [13] T. T. Takahashi, H. Matsufuru, Y. Nemoto and H. Suganuma, Phys. Rev. Lett. **86**, 18 (2001).
- [14] M. A. Shifman, Nucl. Phys. B **173**, 13 (1980).
- [15] R. J. Furnstahl, D. K. Griegel and T. D. Cohen, Phys. Rev. C **46**, 1507 (1992).
- [16] B. J. Harrington and H. K. Shepard, Nucl. Phys. B **124**, 409 (1977).
- [17] D. Diakonov and A. D. Mirlin, Phys. Lett. B **203**, 299 (1988).
- [18] S. i. Nam, J. Phys. G **37**, 075002 (2010).
- [19] T. Schafer and E. V. Shuryak, Rev. Mod. Phys. **70**, 323 (1998).
- [20] N. Cardoso and P. Bicudo, Phys. Rev. D **85**, 077501 (2012).
- [21] D. Antonov and H. J. Pirner, Eur. Phys. J. C **55**, 439 (2008).
- [22] A. Majumder, Phys. Rev. C **87**, 034905 (2013).
- [23] H. Liu, K. Rajagopal and U. A. Wiedemann, Phys. Rev. Lett. **97**, 182301 (2006).

- [24] K. J. Eskola, H. Honkanen, C. A. Salgado and U. A. Wiedemann, Nucl. Phys. A **747**, 511 (2005). 461 (2005).
- [25] A. Dainese, C. Loizides and G. Paic, Eur. Phys. J. C **38**,